NANO LETTERS

2008
Vol. 8, No. 11
3989-3992

Self-Arrangement Among Charge-Stabilized Gold Nanoparticles on a Dithiothreitol Reactivated Octanedithiol Monolayer

Anders O. Lundgren,*,† Fredrik Björefors,‡ Linda G. M. Olofsson,† and Hans Elwing†

Department of Cell and Molecular Biology, Interface Biophysics, Göteborg University, SE-405 30 Göteborg, Sweden, and Department of Physics, Chemistry, and Biology, Linköping University, SE-581 83 Linköping, Sweden

Received August 21, 2008; Revised Manuscript Received September 25, 2008

ABSTRACT

Gold surfaces and structures modified with octanedithiol were reacted with dithiothreitol prior to immersion in buffered solutions of charge stabilized gold nanoparticles. The procedure gives a dithiol layer with adequate properties for a homogeneous octanedithiol monolayer and uniform and reproducible gold nanoparticle binding. The distance between the adsorbing particles is controlled by the particle electrostatic interactions and can be carefully tuned by variation of ionic strength. To some extent, long-range ordering occurs among the adsorbed particles. This behavior is facilitated by the particles' small size compared to the Debye screening but also by the homogeneity of the surface modification. The simple character of the system makes it attractive for fabrication of controlled nanoparticle arrays where further chemical and biological modifications are required.

Self-organization of gold nanoparticles on surfaces and 3D structures has attracted a lot of attention because it enables controlled fabrication of very small structures without the use of lithographic techniques. Typically, realization of ordered structures like nanoparticle arrays with defined interparticle distance has been achieved by assembly of alkanethiol or polymer capped particles on nonbinding substrates upon solvent evaporation or application of electric fields.[1−3] In this letter, we report results from spontaneous self-arrangement of uncapped, charge stabilized gold nanoparticles (∼10 nm) onto gold surfaces modified with a homogeneous dithiol layer. Because these particles are smaller or comparable with the Debye-screening, their adsorption is controlled by electrostatic interactions rather than geometric surface exclusion effects.[4,5] Emphasizing control of electrostatic particle interactions by careful variation of ionic strength and the properties of the adsorbing surface by introduction of a new surface chemical protocol, our scope is to control the surface structure and especially the particle separation. This straightforward and experimentally simple approach proves to be an excellent way to obtain large and stable 2D arrays of uniformly distributed nanoparticles with a tuneable interparticle distance; in agreement with classical DLVO theory,[6] we here demonstrate particle to particle surface distances ranging from 5 to 25 nm. The "pure" character of the system, excluding the need for thiol or polymeric spacers in between the particles, makes it feasible for applications where further chemical and biological modifications of the particles are required.

The adsorption of charged polymeric particles onto surfaces and the influence of electrostatic repulsion between particles on the adsorption process have been extensively described experimentally and theoretically in the literature.[5,7,8] Particles, ranging from 40 to several hundreds of nanometers in diameter, adsorbed directly onto unmodified mineral substrates with opposite charge were found to organize with a short-range order and in some cases also with more extended ordering as a response to different double-layer screening. Later, the use of similar systems of adsorbed polymer particles has been recognized as an important tool in different lithographic processes in order to cover large areas with uniformly distributed dots or pits, a process referred to as colloidal lithography.[9,10] The concept of electrostatic screening controlled adsorption has recently also been demonstrated for smaller entities; Kooij[11] rationalized ionic strength dependent binding of negatively charged gold nanoparticles onto aminosilane modified silicon surfaces, and

* Corresponding author. E-mail: anders.lundgren@gu.se. Phone: +46(0)31 786 2584. Fax: +46(0)31 786 2599.
† Göteborg University.
‡ Linköping University.

10.1021/nl802543g CCC: $40.75
Published on Web 10/18/2008

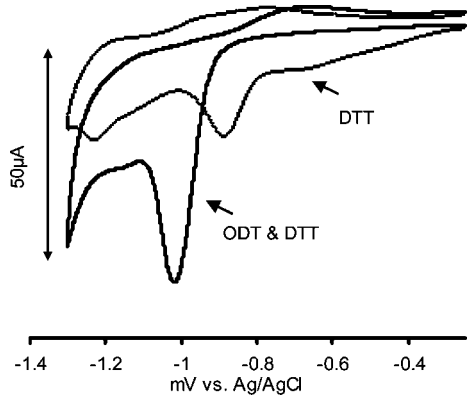

Figure 1. Cyclic voltammogram, first reductive sweep from 0 to −1.3 V vs Ag/AgCl on gold surfaces modified with octanedithiol (ODT) and subsequently reacted with dithiothreitol (DTT) and reference surfaces modified with DTT only. The voltammogram was obtained in 100 mM KOH at a sweep rate of 200 mV/s.

Pericet-Camara[12] showed similar results for positively charged dendrimers on surfaces with different negative charge. Interestingly, it was shown that better organization could be obtained among the dendrimers when the surface charge was reduced. Compared to the results of Kooij, as well as other approaches to gold nanoparticle arrays prepared on silanized glass or silicon,[13,14] the uncharged dithiol modified gold surfaces demonstrated here give rise to shorter interparticle distance, higher structural ordering, and fewer surface bound aggregates among the adsorbed particles. In fact, the patterns formed among the gold nanoparticles on the dithiol interface show the same or better organization as those observed for the larger polymeric colloids on mica surfaces,[7,8] suggesting that the overall homogeneity of the system at the nanolevel and especially the molecular order within the dithiol monolayer is a key factor for the successful particle organization.

Dithiols have been widely used to attach gold nanoparticles to surfaces and structures,[15] however dithiol molecules are prone to form poorly organized multilayers, intralayer disulfides and sulfur oxide compounds during self-assembly,[16,17] and the modified surfaces often display uneven and irreproducible nanoparticle binding. Therefore, to obtain a much more homogeneous dithiol monolayer, the sample surfaces were reacted with reducing dithiotreitol (DTT)[18] after immersion in the octanedithiol (ODT) solution. This procedure gives a dithiol layer with high and reproducible gold nanoparticle binding and adequate properties for an octanedithiol monolayer as determined from ellipsometry and voltammetry. The ellipsometric thickness was determined to 12.8 ± 0.4 Å, which is a reasonable value for the monolayer thickness regarding the molecular length.[16,19] In the voltammetric desorption studies, the charge transfer associated with the reductive desorption of chemisorbed dithiols from the gold surface can be monitored and the thiol surface coverage estimated by integration of the charge under the reductive peaks. Furthermore, the peak positions in the cyclic voltammogram also reflect the molecular interaction within the layer, e.g., molecular packaging and thiol end group functionality.[20] A representative cyclic voltammogram, first reductive and oxidative scan, is presented in Figure 1 above.

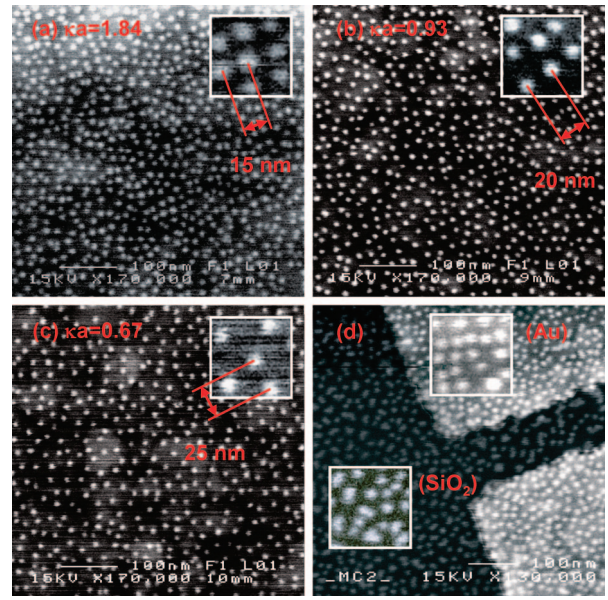

Figure 2. (a−c) Scanning electron microscopy pictures of octanedithiol modified gold surfaces with gold nanoparticles immobilized from citrate buffered solutions with decreasing ionic strength. (d) Gold nanoparticles adsorbed to a silicon substrate with gold patches modified with mercaptopropyl trimethoxy silane and octanedithiol respectively.

Surfaces modified with octanedithiol and then reacted with dithiothreitol display one main reductive peak that can be seen centered at −1015 ± 6 mV with a total integrated charge after reduction for double-layer charging[21] corresponding to 95 ± 6 μC/cm^2. This is close to or slightly above the usually accepted value 85 ± 10% μC/cm^2 corresponding to a full (mono)thiol monolayer.[22] Carot et al. received similar results for the reductive desorption of an octanedithiol monolayer, however, they noted an even higher value for the charge, ∼110 μC/cm^2. This increase in charge for the dithiol layer compared to the monothiol layer was explained by the presence of intralayer disulfide bonds. As a reference, surfaces immersed in only the dithiothreitol solution were examined as well. The dithothreitiol layer adsorbed to these surfaces was found to have an ellipsometric thickness of 6.7 ± 4 Å, i.e., significantly thinner than the octanedithiol treated surfaces. The cyclic voltammogram for desorption of dithiothreitol also appeared more complex compared to that for octanedithiol treated surfaces, displaying several smaller peaks and shoulders. The total integrated charge, 37 ± 17 μC/cm^2, indicates submonlayer coverage. This is in agreement with results by others, indicating that dithiothreitol layers are disordered and that dithiothreitol binds to the surfaces with both sulfur functionalities.[23] Cyclic voltammetry on surfaces treated with only dithiothreitol showed no interfering peaks with the dithiolthreitol treated octanedithiol layers. Altogether, the results from ellipsometry and voltammetric desorptions measurements strongly indicate that the surfaces treated with octanedithiol and subsequently dithiothreitol acquire well organized octanedithiol monolayers rather than that the octanedithiol is exchanged for dithiothreitol.

Immobilization of gold nanoparticles on the dithiol modified surfaces was done by incubation in a citrate buffered gold sol. The gold nanoparticles (radius $a = 4.85 \pm 0.35$ nm) were prepared from citrate reduction of $HAuCl_4$ with addition of tannic acid as an extra reductive agent.[24] All gold sols had a constant particle concentration of 5.5×10^{-8} M but different ionic strength. The latter was obtained via dilution of a 10 mM pH 4.0 citrate buffer stock solution with ultrapure water (18.3 MΩ cm), whereupon ionic composition, Debye screening length, κ^{-1}, and the dimensionless screening parameter, κa was calculated for each solution. The weakly acidic buffer was chosen in order to suppress charging of the sulfhydryl groups at the surface but also with respect to the stability of the gold sols. It should be noted that all gold sols are not thermodynamically stable and that signs of particle aggregation was visible within 24 h for the sol with the highest ionic strength.

The surfaces were analyzed with scanning electron microscopy, and representative pictures of surfaces incubated in gold sols with different ionic strength are presented in Figure 2a−c. The particle surface coverage was estimated by manual counting, and values for the mean particle center to center distance R for each surface were obtained from calculations of radial distributions $g(r)$, where r is the distance from the particle center, Figure 3a. All surfaces were found to bind particles in a uniform manner with very few particle aggregates. In the radial distribution, this was manifested by the primary peak, representing the most probable distance between adjacent particles, i.e., $r = R$, and the following smaller peaks, which suggests a certain degree of localized long-range ordering among the adsorbed particles.[4,5]

The surface coverage and interparticle distance clearly depend on the ionic strength with diminishing coverage for lower ionic strength, Figure 3b. Applying the model introduced by Adamczyk,[5] the spatial extension of the particle interactions at the surface can be estimated from DLVO theory by assigning each particle an effective hard sphere radius, a_{eff}, calculated according to eq 1.[8,11,25]

$$U_{pp}(2a_{eff})/kT = 1/\lambda \tag{1}$$

where $U_{pp}(r)$ is the pairwise particle interaction potential, kT the thermal energy (defined by the Boltzmann constant k and the temperature T), and λ is a constant. Assuming random sequential adsorption (RSA), the observed surface coverage θ_{eff} then relates to the effective hard sphere radius through the relation 2.[5]

$$\theta_{eff} = \theta_{jam}(a/a_{eff})^2 \tag{2}$$

where $\theta_{jam} = 0.547$ is the surface coverage at the saturation limit for RSA of real hard spheres.

Experimental values obtained for the interparticle distance R appear to be comparable to modeled values of $2a_{eff}$ from 1, with U_{pp} being the sum of repulsive electrostatic interactions using a linear spherical approximation 3[26] valid for small κa and attractive Van der Waals interactions according to eq 4.

$$U_{rep} = 4\pi a^2 Y^2 \left(\frac{kT}{e}\right)^2 \frac{1}{r} e^{-\kappa(r-2a)},$$

$$Y = 8\tan h\left(\frac{e\psi_0}{4kT}\right) \frac{1}{1+\sqrt{1-\frac{2\kappa a+1}{(\kappa a+1)^2}\tan h^2\left(\frac{e\psi_0}{4kT}\right)}} \tag{3}$$

$$U_{attr} = -\frac{A_H}{6}\left(\frac{2a^2}{r^2-4a^2} + \frac{2a^2}{r^2} + \ln\frac{r^2-4a^2}{r^2}\right) \tag{4}$$

Calculations were done numerically, solving 3 with a constant surface potential $\Psi_0 = -50$ mV,[27−29] Hamaker constant $A_H = 2.5 \times 10^{-19}$ J[27] and $\lambda = 1.44$[30,31] as input parameters. Comparison of real and modeled surface coverage by insertion of the calculated a_{eff} into 2 reveals that the real surface coverage is higher than expected from the effective hard sphere approximation. A probable explanation to this discrepancy is the existence of areas with a higher degree of order than expected from RSA of hard spheres, giving a somewhat higher value of θ_{jam}. Similar tendencies to ordering have earlier been observed for much larger polymeric colloids adsorbed from solution with very low ionic strength,[7] i.e., $\kappa a \approx 1$ or lower, which is the same as

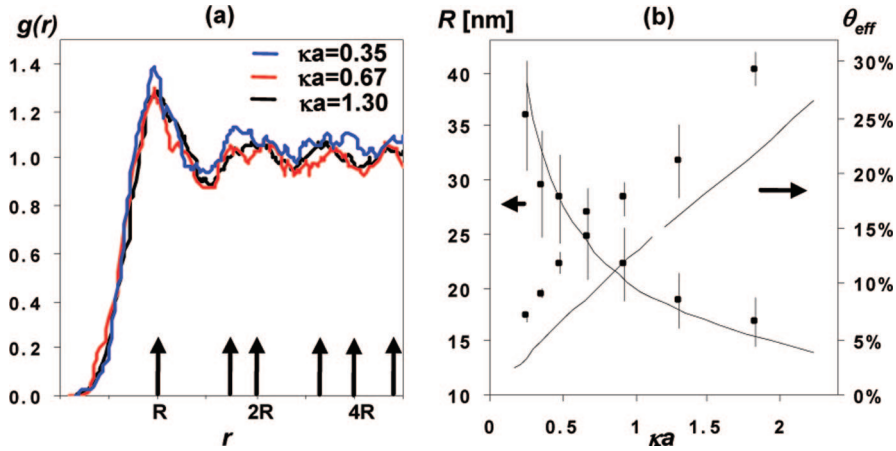

Figure 3. (a) Radial distribution functions calculated from SEM pictures. The radial distance is scaled by the interparticle distance R for comparison of different buffers. Arrow insets denote peak positions in a close packed configuration. (b) Experimental values (squares) for particle center to center separation and particle surface coverage and modeled values (lines) for effective hard sphere radius according to eq 1 and surface coverage according to eq 2 as function of the screening parameter κa.

for the gold nanoparticle solutions used here. A general trend for more surface organization with decreasing κa has also been shown in Brownian dynamics simulations on adsorption of charged particles, however, in these simulations, surface diffusion of particles was allowed.[4]

Silanes containing NH_2 or SH functional groups have been widely used to create self-assembled gold nanoparticle monolayers on glass or silicon surfaces.[11,13,15] Therefore, to estimate the influence from the binding layer on particle binding and structure, a silicon surface with lithographically defined gold patterns were treated first with octanedithiol and subsequently with mercaptopropyl trimetoxy silane (MPTMS). By this procedure, both gold and silicon oxide areas on the surface were provided with the same particle binding functionality (−SH), but their distribution on the surface differ due to the organizing properties of the molecules.[1] Figure 2d shows such a surface after incubation in gold sol. It was found that the MPTMS-modified silicon dioxide surfaces bound approximately 30% less particles compared to the dithiol modified gold surfaces. Particles on MPTMS also appeared less homogenously distributed, which was also the case when comparing with those gold nanoparticle arrays prepared on silanized glass or silicon present in the literature.[11,13]

In conclusion, we have shown that gold nanoparticles self-assembled onto a homogeneous dithiol monolayer can arrange in a controllable fashion due to particle electrostatic interactions. The interparticle distance can be predicted by DLVO theory, and very small interparticle distances can be achieved by self-assembly of particles from destabilized solutions, i.e., when Van der Waals forces have substantial influence on the particle interactions. Local tendencies toward long-range ordering can be seen among the bound particles. Such an ordering is probably governed by the particles' small size but also by the superior homogeneity and reactivity of the surface modification. We suggest the method for applications where further chemical and biological modifications of the arrays are required; immobilized particles remain stable in position and readily bind thiols or biomolecules, whereas unreacted dithiols can be blocked with for example maleimide conjugated polyethylene glycol (Supporting Information).

Acknowledgment. Bo Liedberg and Mattias Brust are gratefully acknowledged for fruitful discussions and valuable advice. This research was realized within NACARDIO, a research program funded by the European Union.

Supporting Information Available: Details of experimental procedures, additional SEM pictures, details of modeling, and data on the binding of maleimide-PEG in between particles. This material is available free of charge via the Internet at http://pubs.acs.org.

References

(1) Spatz, J. P.; Roescher, A.; Möller, M. *Adv. Mater.* **1996**, *8*, 337–340.
(2) Giersig, M.; Mulvaney, P. *Langmuir* **1993**, *9*, 3408–3413.
(3) Kiely, C. J.; Fink, J.; Brust, M.; Bethell, B.; Shiffrin, D. J. *Nature* **1998**, *396*, 444–446.
(4) Gray, J. J.; Bonnecaze, R. T. *J. Chem. Phys.* **2001**, *114*, 1366–1381.
(5) Adamczyk, Z.; Zembala, M.; Siwek, B.; Warszynski, P. *J. Colloid Interface Sci.* **1990**, 140.
(6) Verwey, E. J. W.; Overbeek, J. T. G., *Theory of the Stability of Lyophobic Colloids*; Elsevier Publishing Company Inc.: Amsterdam, 1948.
(7) Johnson, C. A.; Lenhoff, A. M. *J. Colloid Interface Sci.* **1996**, *179*, 587–599.
(8) Semmler, M.; Mann, E. K.; Ricka, J.; Borkovec, M. *Langmuir* **1998**, *14*, 5127–5132.
(9) Hanarp, P.; Sutherland, D. S.; Gold, J.; Kasemo, B. *Colloids Surf., A* **2003**, *214*, 23–36.
(10) Michel, R.; Reviakine, I.; Sutherland, D. S.; Fokas, C.; Csucs, G.; Danuser, G.; Spencer, N. D.; Textor, M. *Langmuir* **2002**, *18*, 8580–8586.
(11) Kooij, E. S.; Brouwer, E. A. M.; Wormeester, H.; Poelsema, B. *Langmuir* **2002**, *18*, 7677–7682.
(12) Pericet-Camara, R.; Cahill, B. P.; Papastavrou, G.; Borkovec, M. *Chem. Commun.* **2007**, 266–268.
(13) Freeman, R. G.; Grabar, K. C.; Alison, K. J.; Bright, R. M.; Davis, J. A.; Andrea, P. G.; Hommer, M. B.; A., J. M.; Smith, P. C.; Walter, D. G.; Natan, M. J. *Science* **1995**, *267*, 1629–1632.
(14) Grabar, K. C.; Smith, P. C.; Musick, M. D.; Davis, J. A.; Walter, D. G.; Jackson, M. A.; Guthrie, A. P.; Natan, M. J. *J. Am. Chem. Soc.* **1996**, *118*, 1148–1153.
(15) Daniel, M.; Asruc, D. *Chem. Rev.* **2004**, *104*, 293–346.
(16) Kohli, P.; Taylor, K. K.; Harris, J. J.; Blanchard, G. J. *J. Am. Chem. Soc.* **1998**, *120*, 11962–11968.
(17) Carot, M. L.; Esplandiu, M. J.; Cometto, F. P.; Patrito, E. M.; Macagno, V. A. *J. Electroanal. Chem.* **2005**, *579*, 13–23.
(18) Cleland, W. W. *Biochemistry* **1964**, *3*, 480–482.
(19) Ohgi, T.; Sheng, H.-Y.; Nejoh, H.; Dong, Z.-C.; D., F. *Appl. Phys. Lett.* **2001**, *79*, 2453–2455.
(20) Bard, A. J.; Rubinstein, I., *Electroanalytical Chemistry*; Marcel Dekker Inc: New York, 1996; Vol. 19.
(21) Yang, D.-F.; Wilde, C. P.; Morin, M. *Langmuir* **1996**, *12*, 6570–6577.
(22) Zhong, C.-J.; Porter, M. D. *J. Electroanal. Chem.* **1997**, *425*, n/a.
(23) MacDairmid, A. R.; Gallagher, M. C.; Banks, J. T. *J. Phys. Chem. B* **2003**, *107*, 9789–9792.
(24) Slot, W. J.; Geuze, H. J. *J. Cell Biol.* **1981**, *90*, n/a.
(25) Russel, W. B.; Saville, D. A.; Schowalter, W. R., *Colloidal Dispersions*; Cambridge University Press: Cambridge, 1989.
(26) Ohshima, H.; Healy, T. W.; White, L. R. *J. Colloid Interface Sci.* **1982**, *90*, 17–26.
(27) Kim, T.; Lee, K.; Gong, M.-s.; Joo, S.-W. *Langmuir* **2005**, *21*, 9524–9528.
(28) Kunze, J.; Burgess, I.; Nichols, R.; Buess-Herman, C.; Lipkowski, J. *J. Electroanal. Chem.* **2007**, *599*, 147–159.
(29) Brewer, S. H.; Glomm, W. R.; Johnson, M. C.; Knag, M. K.; Franzen, S. *Langmuir* **2005**, *21*, 9303–9307.
(30) Russel et al. showed theoretically for particles in solution that $1 < \lambda < e$; here we use the intermediate value 1.44.
(31) Vanderberg, E.; Bertilsson, L.; Liedberg, B.; Uvdal, K.; Erlandsson, R.; Elwing, H.; Lundström, I. *J. Colloid Interface Sci.* **1991**, *147*, 103–118.

NL802543G